

Article

Characteristics and Health Risk Assessment of Mercury Exposure via Indoor and Outdoor Household Dust in Three Iranian Cities

Reza Dahmardeh Behrooz ^{1,*}, Mahsa Tashakor ², Reza Asvad ³, Abbas Esmaili-Sari ³ and Dimitris G. Kaskaoutis ^{4,*} 

¹ Department of Environmental Sciences, Faculty of Natural Resources, University of Zabol, Zabol 98615-538, Iran

² School of Geology, College of Science, University of Tehran, Tehran 14155-6455, Iran; mahsa.tashakor@ut.ac.ir

³ Department of Environment, Faculty of Natural Resources and Marine Science, Tarbiat Modares University, Tehran 14115-111, Iran; reza.asvad@gmail.com (R.A.); esmaili@modares.ac.ir (A.E.-S.)

⁴ Institute for Environmental Research and Sustainable Development, National Observatory of Athens, Palaia Penteli, 15236 Athens, Greece; dkask@noa.gr

* Correspondence: dahmardehbehrooz@uoz.ac.ir (R.D.B.); dkask@noa.gr (D.G.K.)

Abstract: This study aims to increase our current knowledge on the concentration of particulate-bound mercury (PBM) in urban environments of three Iranian cities, where high concentrations of dust particles can act as carriers for mercury transport and deposition. A total of 172 dust samples were collected from Ahvaz, Asaluyeh, and Zabol residential houses and in outdoor air and were analyzed for total mercury content. Ahvaz is a highly industrialized city with large metallurgical plants, refineries, and major oil-related activities, which were assumed to contribute to elevated contents of PBM in this city. Very high levels of Hg contamination in Ahvaz indoor dust samples were calculated (Contamination Factor: CF > 6). Sampling sites in Asaluyeh are influenced by Hg emissions from the South Pars Gas Field. However, the results revealed a relatively lower concentration of PBM in Asaluyeh, with a low-to-moderate level of Hg contamination. This is likely ascribed to the lower content of total mercury in hydrocarbon gases than crude oil, in addition to the absence of metal smelting plants in this city compared to Ahvaz. Zabol, as a city devoid of industrial activity, presented the lowest levels of PBM concentration and contamination. Indoor dust in Ahvaz showed considerable potential to cause a non-carcinogenic health risk for children, mainly through the inhalation of PBM, while the health risk for other cities was below safe limits. The trend of health risk was found in the order of indoor > outdoor and children > adults in all studied cities.

Keywords: mercury; dust; metallurgical plants; refineries; risk assessment; Iranian cities



Citation: Dahmardeh Behrooz, R.; Tashakor, M.; Asvad, R.; Esmaili-Sari, A.; Kaskaoutis, D.G. Characteristics and Health Risk Assessment of Mercury Exposure via Indoor and Outdoor Household Dust in Three Iranian Cities. *Atmosphere* **2022**, *13*, 583. <https://doi.org/10.3390/atmos13040583>

Academic Editors: Rosa Caggiano and Antonio Speranza

Received: 7 March 2022

Accepted: 1 April 2022

Published: 5 April 2022

Publisher's Note: MDPI stays neutral with regard to jurisdictional claims in published maps and institutional affiliations.



Copyright: © 2022 by the authors. Licensee MDPI, Basel, Switzerland. This article is an open access article distributed under the terms and conditions of the Creative Commons Attribution (CC BY) license (<https://creativecommons.org/licenses/by/4.0/>).

1. Introduction

Urban dust is a complex heterogeneous mixture of organic and inorganic non-metallic and metallic solid particles of various origins [1,2]. It is composed of naturally occurring substances (weathered rocks, eroded soil particles, plant litters, etc.), as well as anthropogenic particles mainly released from industries, vehicles, houses, and urban infrastructure [3,4]. Dust is an important medium in a city's atmosphere, hosting various air pollutants, including potentially toxic elements (PTEs) loosely bound to the surface of dust particles [5,6]. As a result of rapid urbanization and industrial development, the emission and deposition of PTEs increased in many urban environments throughout the world. Exposure to PTEs through urban dust can threaten the ecosystem and cause a wide range of adverse health effects for city dwellers [7]. Dust can also accelerate environmental pollution by suspending and transporting particulate-bound PTEs; hence, it is considered a key pertinent indicator of urban environmental quality and human health [8,9]. PTEs have frequently been investigated in the soil and street dust of numerous cities around the globe [10–14]. The focus, however, has mainly been on typical urban elements, such as Pb, Cd, Cu, and Zn [15–17], while mercury (Hg) as a hazardous contaminant has received less attention.

Mercury is a non-essential toxic element that may pose health impacts even at very low concentrations [18,19]. This element is listed as a priority by many international agencies, such as UNEP, WHO, and FAO [20]. Even though sources of Hg can be natural (e.g., geochemical anomalies, volcanoes, forest wildfires), anthropogenic factors are responsible for the largest portion of Hg emissions in the environment [21,22]. Due to the accelerating pace of industrialization and its by-products, the levels of Hg on a global scale have constantly increased in recent decades, compared to the natural contributions [23,24]. The emission levels of Hg have reached up to 24 times higher today than those before the industrial period [25,26]. Mining and nonferrous metal production, chemical, and pharmaceutical industries, coal combustion, municipal solid waste incineration, and cement production plants contribute significantly to atmospheric Hg input [27–31].

Atmospheric Hg can be categorized into three defined forms: gaseous elemental mercury (GEM)-Hg⁰, reactive gaseous mercury (RGM)-Hg², and particulate-bound mercury (PBM) [32]. Particulate-bound mercury plays an important role in biogeochemical cycling, even if it is not the predominant constituent of total Hg in ambient air [33–35]. PBM is of prevalent concern due to its high deposition velocity and scavenging coefficients, which lead to its natural wet and dry settlement to the ground [36,37]. On the other hand, through adsorption onto the particle surface, gaseous phase mercury precipitates in terrestrial and aquatic ecosystems [38,39]. PBM can be transported at long distances or be set down near the source, depending on meteorological conditions, particularly wind speed and humidity, particle size, and deposition rate [40].

The association of particulate matter and Hg with health issues, including neurological and behavioral disorders, cancer, and mortality, is well documented [41–43]. Hg contaminants in urban dust can enter the human body through swallowing, breathing, and dermal adsorption and can cause health problems, especially in children [44,45]. About 80% of inhaled elemental mercury remains in body organs (ATSDR, 1999).

Some scholars believe that respirable particulate matter in indoor air is a more important source of exposure to Hg and the occurrence of health issues than outdoor atmospheric particles [46,47]. It is argued that people, and in particular apartment-dwelling inner-city children, spend more time at home, where outdoor dust entering through doors, windows, etc., is added to household dust from various residents' activities [48,49]. Air conditioner filter dust is assumed to be representative of particulate matter (PM) in indoor air [50]. When air passes through the air conditioning systems, the re-suspended particles from the settled dust on the surfaces of food, skin, toys, and furniture are attached to the filters to improve the indoor air quality [51].

Several studies have analyzed the PTEs from soil and airborne dust in Iranian cities or in heavily industrialized areas, also providing estimates of health risk assessment [52–56]. However, much less attention has been given to Hg emissions and concentrations in urban and industrialized areas in Iran [57,58]. This study provides an analysis of the content of particulate-bound mercury (PBM) in urban outdoor and indoor household dust from three Iranian cities with different characteristics regarding their industrial and dusty background, i.e., Ahvaz, Asaluyeh, and Zabol. Household and ambient air pollution by PBM was assessed to explore where the investigated cities stand, compared to other urban sites. Moreover, this study evaluates the residents' health risks from prolonged exposure to PBM via dust (outdoor and indoor) through the inhalation, ingestion, and dermal contact pathways both for children and adults.

2. Study Areas

This study was conducted in three polluted Iranian cities, namely Ahvaz (31°19' N and 48°41' E) in the southwest, Asaluyeh (27°28' N and 52°36' E) in the south, and Zabol (31°01' N and 61°29' E) in the east. The study areas and the locations of the sampling sites are shown in Figure 1. These sites were chosen for their different pollution characteristics. Ahvaz, as the largest city in southwest Iran, is highly impacted by vehicle emissions, industrial activity, and dust storms [59,60]. Asaluyeh is a medium-sized city with a

nearby high industrial area [57], and Zabol is highly impacted by dust storms during the summer season [55].

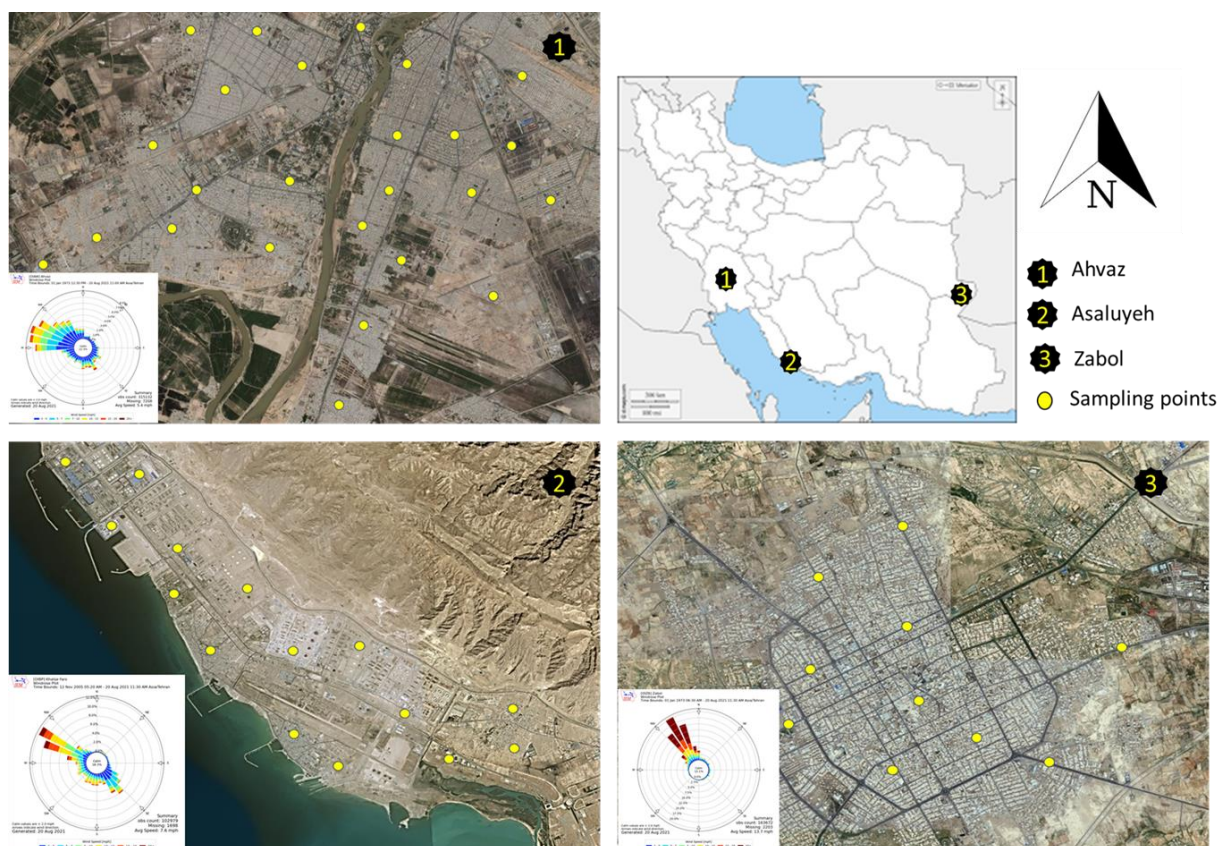


Figure 1. Study areas and the location of sampling sites in Ahvaz (1), Asaluyeh (2), and Zabol (3). The wind speeds and dominant direction at each site are also plotted in insert graphs. Data taken from meteorological stations at each site.

Ahvaz city, with a population of about 1.32 million (census 2016), is located in the center of Khuzestan province, an oil-producing province in southwest Iran. Ahvaz is a historical city and capital of ancient civilizations built on the banks of the Karoon River. Ahvaz has an arid climate with an average annual rainfall of about 213 mm and an average temperature of 25 °C. The prevailing wind direction is from the west/northwest (Figure 1). Nowadays, Ahvaz has emerged as an important, highly industrial city with numerous oil-related operations and large metal smelting plants. Ahvaz is surrounded by numerous oil wells belonging to the Ahvaz and Ramin oil fields operated by the National Iranian South Oil Company (NISOC), National Iranian Drilling Company (NIDC), Khuzestan Steel Company (KSC), and many other metallurgical and petrochemical plants. On the other hand, Ahvaz is located downwind of frequent and severe dust storms originating from the vast deserts of the Arabian Peninsula, Iraq, and Syria [59–61]. The combination of dust storms and urban/industrial emissions results in a severe deterioration of air quality and can pose an important human health risk, rendering Ahvaz one of the most polluted cities in the world [62–64].

Asaluyeh is a coastal town in south Iran, known as one of the most heavily industrialized areas in the world, with several gas and petrochemical industries and the most important oil refineries in Iran. This area is like a narrow strip of land located between the Persian Gulf and the Zagros Mountains (Figure 1). It is situated ~300 km from the southeast of Bushehr city and has about 70,000 residents. The sampling sites in Asaluyeh were selected in the South-Pars region, the most industrial and residential area (Figure 1). The south Pars Economic Exclusive Zone is a core area of 14,000 ha, hosting huge petro-

chemical complexes of various plants and refineries and is the closest land point to one of the world's largest natural gas fields, the South Pars Gas Field [57]. It comprises 16 gas processing plants, 15 petrochemical complexes, and their downstream industries. In addition, the arid zones surrounding this area are sources of desert dust, which may also be long-range transported over Asaluyeh via strong northwesterlies (Shamal) throughout the year, with higher frequency in spring and summer [65].

Zabol is located in the northeastern part of Sistan and Baluchestan province, in East Iran, with a population of 166,448 people (census 2016). Zabol is not an industrial city, and its economy is based on agricultural activities in the surrounding fields that are fed by the Hamoun lakes complex, Hirmand River, and its tributaries [66,67]. It has a hot and dry desert climate with an average temperature of 23 °C and average annual precipitation of ~55 mm. Zabol is exposed to a high volume of dust particles throughout the year, but mostly during the summer dusty period, under the influence of a violent northern wind (Levar or 120-day wind) [68]. Zabol is characterized by poor air quality as a result of frequent and intense dust storms, and is considered among the most polluted cities over the globe in terms of dust particulate matter [69,70].

During the sampling periods (spring–summer), winds were mostly from west/northwest directions in all cities (Figure 1), representing the Shamal regime in Ahvaz and Asaluyeh and the Levar regime in Zabol. Previous studies analyzing air-mass back trajectories identified the Iraqi plains and arid/desert regions in northeast Arabian Peninsula as the main sources of dust in Ahvaz [60] and the Hamoun dried beds as the major sand/dust source for Zabol [67]. However, trace elements, which may be contaminated and transported with dust, may have a different origin, i.e., from local sources, oil refineries, and combustion emissions, which are very difficult to quantify.

3. Material and Methods

3.1. Sample Collection and Preparation

A total of 172 household and outdoor settled dust samples were collected from Ahvaz ($n = 36$), Asaluyeh ($n = 30$), and Zabol ($n = 20$) during spring (April–May 2019), and the same number of samples in each city was repeated during the summer (June to August 2019). These are the hottest days of the year when the use of air conditioning for domestic cooling is maximized. The household total suspended particles (TSP) were collected on split air conditioner filters from a total of 86 residences (1 sample per each) at random district zones. The surveyed residences were private dwelling units selected based on landlords' willingness to participate in this study. An effort was made to choose houses with the minimum of major indoor particle sources, such as smokers, coal, and oil furnaces, etc. All air conditioners were wall-mounted, and the majority were installed in the living rooms. The place of the installations, close to balcony doors or windows, did not show any meaningful influence. Prior to sampling, filters were unfastened from the units and thoroughly washed by submerging in a volume of water mixed with a small amount of mild detergent or liquid soap. The filters were soaked for 1 h, thoroughly rinsed, and air dried before fixing back. After that, dust particles were gently brushed from the filter screens onto clean papers and then placed into plastic sealed labeled bags.

At each site, within 10–50 m of the houses, the exterior dust samples were passively taken from the deposited particles on flat plastic containers laid at a height of 1.5 m above the ground. According to Del Rio-Salas et al. [71], only the particles suspended at elevations below 3 m contribute to the exposure paths of elements to the human body. Throughout the sampling periods, the meteorological conditions were steady, without strong wind and precipitation. Dust samples were swept into polyethylene sealed bags with fingers wearing powder-free gloves after removal of any visible debris, grit, or hair. Samples were then transferred to the laboratory and stored at a temperature below 5 °C until analysis.

3.2. Analytical Procedures

About 25 to 50 mg of each dust sample was weighed and then analyzed to measure the amount of mercury using an AMA 254 Mercury Analyzer (Leco Corporation, Agilent Tech, CA, USA), for which no previous chemical digestion is requested. Ultrapure oxygen was used as a carrier gas with an inlet pressure of 250 kPa and a flow rate of 200 mL/min. Each sample was analyzed in triplicate.

Instrument calibration was performed with a NIST-traceable Hg solution (AccuTrace Single Element Standard; AccuStandard Inc., New Haven, CT, USA). Seven replicate analyses of standard reference materials, SRM 1633b (Constituent Elements in coal fly ash), SRM 2709 (San Joaquin Soil Baseline Trace Element Concentrations), and SRM 2711 (Montana II soil), were used to verify the reliability of the analysis. The accuracy of SRM measurements was found to range between 96% and 108%, with a relative standard deviation (RSD) < 13%. To prevent the carry-over effect, at least one procedural blank was analyzed after three replicates of the same sample. The method detection limit (LOD) was estimated at 0.3 ng/g dry weight (dw) for all considered matrices. The limit of quantification (LOQ) of the proposed method was calculated in blank samples as 3-fold of the average blank concentrations and set at 1 ng/g dry weight (dw). The accuracy of the replicate analysis is shown in Table 1.

Table 1. Results of the quality assurance procedure for mercury analysis ($\mu\text{g/g}$).

	Certified Value	Our Results	Accuracy
NIST-1633	0.141	0.153	+8.5%
NIST-2709	1.400	1.455	+3.9%
NIST-2711	6.250	6.011	−3.9%

NIST: National Institute of Standard and Technology.

3.3. Statistical Analysis

The geochemical results were analyzed for descriptive statistics using Microsoft Excel and SPSS 23.0 software. The Kolmogorov–Smirnov test was carried out to control the normality assumption of the data. A non-parametric Mann–Whitney U test was applied to determine the difference in Hg concentration between the outdoor and indoor samples and those taken during the spring and summer periods.

The single index of the Contamination Factor (*CF*) was calculated as an indicator of pollution [72]. This widely used geochemical criterion is the quotient of concentration of each element in a sample (*C_n*) and the concentration of the same element in the reference soil (*B_n*):

$$CF = C_n / B_n$$

In this study, the world average concentration of Hg in uncontaminated soils (0.07 mg/Kg) given by Kabata-Pendias [73] was used as a reference value. According to the degree of pollution, *CF* is classified into four classes, from unpolluted to very polluted, as below [74]:

- $CF < 1$ low contamination;
- $1 \leq CF < 3$ moderate contamination;
- $3 \leq CF < 6$ considerable contamination;
- $CF \geq 6$ very high contamination.

3.4. Human Health Risk Assessment

3.4.1. Exposure Assessment

The degree of non-cancer risk associated with particulate-bound Hg in indoor and outdoor dust samples was assessed using the health-risk assessment model introduced by the U.S. Environmental Protection Agency (USEPA) [75]. This model evaluates the probability of health issues based on the level of exposure to risk factors through the three main pathways of ingestion, inhalation, and dermal contact [15,76]. This study also investigated respiratory exposure in two susceptible groups of residents: adults (up to

the age of 70 years) and children (up to the age of 15 years). The average daily intakes of mercury via the pathways of ingestion (ADI_{ing}), inhalation (ADI_{inh}) and dermal contact (ADI_{drm}) were calculated using Equations (1)–(3):

$$ADI_{ing} = C_s \times \frac{IngR \times EF \times ED}{BW \times AT} \times 10^{-6} \quad (1)$$

$$ADI_{inh} = C_s \times \frac{InhR \times EF \times ED}{PEF \times BW \times AT} \quad (2)$$

$$ADI_{drm} = C_s \times \frac{ESA \times SAF \times DAF \times EF \times ED}{BW \times AT} \times 10^{-6} \quad (3)$$

where C_s is the total concentration of Hg in the dust samples (mg kg^{-1}); $IngR$ is ingestion rate (mg/d), 100 for adults and 200 for children; EF is exposure frequency, 350 days/year; ED is exposure duration, 30 years for adults and 6 years for children; BW is body weight, 70 kg for adults and 15 kg for children; AT is averaging time (d), 10,950 for adults and 2190 for children; ESA is exposed surface area (cm^2), 5700 for adults and 2800 for children; SAF is skin adherence factor (mg/cm^2), 0.07 for adults and 0.2 for children; DAF is dermal absorption factor (unitless), 10^{-3} for adults and children; $InhR$ is inhalation rate (m^3/d), 20 for adults and 7.6 for children [77]; PEF is particle emission factor, $1.36 \times 10^9 \text{ m}^3 \text{ kg}^{-1}$ (USEPA [75]).

3.4.2. Non-Carcinogenic Risk Assessment

Non-carcinogenic hazards of a single element are defined as the hazard quotient (HQ), which is calculated by dividing the average daily intakes by a specific reference dose (Equation (4)):

$$HQ_e = \frac{ADI_e}{RfD} \quad (4)$$

where RfD is the reference dose (mg/kg/day), an estimation of the maximum allowable level of an element that has no hazardous impact on human health, and e represents the pathway. The reference doses for mercury used in the analysis were taken from the USEPA [75], which are 1.6×10^{-1} for direct ingestion, 3.20×10^{-2} for dermal absorption, and 2.86×10^{-6} for inhalation. The overall risk using the Hazard Index (HI) is obtained by summing the hazard quotients for each pathway (Equation (5)). According to the USEPA [75], when the HQ or HI value is <1 , adverse health effects are unlikely to be experienced by residents. Whereas $HQ > 1$ indicates the potential of non-carcinogenic health effects, with an increasing probability as the HQ increases [78,79].

$$HI = \sum HQ_e = \sum \frac{ADI_e}{RfD} \quad (5)$$

Due to the lack of a carcinogenic slope factor (SF) for Hg, the carcinogenic risk was not estimated.

4. Results and Discussion

4.1. Total Concentration of PBM in Urban Dust

Descriptive statistics of mercury concentrations (mg kg^{-1}) in indoor and outdoor dust of the three urban areas are shown in Table 2. The skewness and kurtosis inspection demonstrated that the Hg concentrations in the indoor and outdoor dust of Ahvaz and Asaluyeh do not follow a normal distribution. This was confirmed by the Kolmogorov–Smirnov (K-S) normality test (p value < 0.05). The non-normal distribution might reflect the influence of diverse anthropogenic factors. In contrast, the distribution of Hg data in Zabol dusts, both indoor and outdoor, was found to be mostly normal (K–S $p > 0.05$). This may be an indication of a uniform source for Hg in Zabol, without the presence of specific hot spots of Hg or outliers.

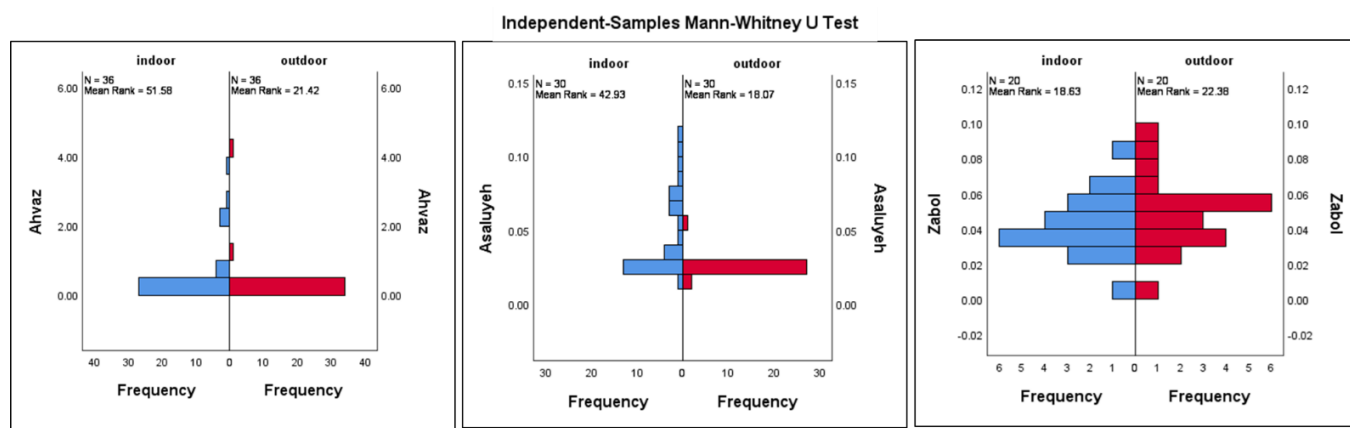
Table 2. Descriptive statistics of mercury concentration (mg kg^{-1}) in urban dust samples in comparison to uncontaminated soils, and the average values in different cities of the world.

Particulate-Bound Mercury (PBM)		Min	Max	Mean	Median	SD	Skewness	Kurtosis
Indoor dust								
	Ahvaz ($n = 36$)	0.04	3.95	0.67	0.37	0.86	2.48	6.04
	Asaluyeh ($n = 30$)	0.01	0.12	0.05	0.03	0.03	1.09	0.13
	Zabol ($n = 20$)	0.01	0.08	0.04	0.04	0.02	0.60	1.82
Outdoor dust								
	Ahvaz ($n = 36$)	0.02	1.06	0.07	0.04	0.17	5.75	33.5
	Asaluyeh ($n = 30$)	0.02	0.26	0.04	0.02	0.01	4.61	23.6
	Zabol ($n = 20$)	0.00	0.06	0.03	0.03	0.02	0.19	0.93
Uncontaminated soil ¹				0.07				
Exterior dusts (street/road/ roadway dusts)				Beijing (China) ²				
				0.34				
				Hamedan (Iran) ³				
				0.15				
				Luanda (Angola) ⁴				
				0.13				
				Nanjing (China) ⁵				
				0.12				
				Kavala (Greece) ⁶				
				0.10				
				Aviles (Spain) ⁷				
				1.20				
				10.80				
				0.002				
				Vanadzor (Armenia) ⁸				
				0.04				
				0.54				
				0.26				
Household dust				Šid (Serbia) ⁹				
				0.005				
				1.56				
				0.13				
				Ottawa (Canada) ¹⁰				
				0.01				
				37.00				
				1.72				

¹ Kabata-Pendias [73]; ² Xinmin, et al. [80]; ³ Modabberri et al. [56]; ⁴ Ferreira-Baptista and De Miguel [81]; ⁵ Hu et al. [4]; ⁶ Christoforidis and Stamatis [82]; ⁷ Ordóñez et al. [42]; ⁸ Sahakyan, et al. [83]; ⁹ Nedić, et al. [84]; ¹⁰ Rasmussen et al. [85].

It was statistically (Mann–Whitney U test) confirmed that the seasonal variation between spring and summer has little effect on the distribution of Hg in indoor and outdoor dust samples (p value > 0.05) in all of the studied areas. Hence, these data were treated together in one group. However, as can be noted from the Mann–Whitney U test (Figure 2), the content of Hg in the indoor dust of Ahvaz and Asaluyeh differs significantly from that in the outdoor dust (p value ~ 0.00). This difference was not identified in Zabol dust, presenting a significance level of about 0.314, suggesting similarity in the Hg contents of both indoor and outdoor samples (Figure 2).

As shown in Table 2, the PBM concentration of indoor dust in Ahvaz ranged from 0.04 to 3.95 mg kg^{-1} with a median of 0.37 mg kg^{-1} , which is about 8.6 times greater than the median Hg concentration for outdoor dust (0.04 mg kg^{-1}) in Ahvaz. The mean indoor Hg concentration is significantly higher (0.67 mg kg^{-1}), indicating episodes of very high Hg levels. A relatively lower PBM concentration was found in Asaluyeh dust samples, ranging from 0.01 to 0.12 mg kg^{-1} (median of 0.03 mg kg^{-1}) in indoor and from 0.02 to 0.26 mg kg^{-1} (median: 0.02 mg kg^{-1}) in outdoor dusts. The concentrations of PBM in all of the analyzed Asaluyeh house dust samples exceeded those of the outdoor samples, with a ratio of 1.26. Higher accumulation of PBM in house (indoor) dust compared to ambient air was also reported in other studies, and was partly attributed to the effect of building materials (e.g., interior decorations, paints, fluorescent lamps) [86] and the affinity of Hg for organic matter [85]. However, the indoor and outdoor dust in Asaluyeh showed fairly similar values of Hg with respect to Zabol, with median concentrations of 0.04 mg kg^{-1} (0.01–0.08 mg kg^{-1}) and 0.03 mg kg^{-1} (0.00–0.06 mg kg^{-1}), respectively.



Hypothesis Test Summary- Independent-Samples Mann-Whitney U Test			
	Null Hypothesis	Sig.	Decision
1	The distribution of Ahvaz is the same across categories of VAR1.	0.000	Reject the null hypothesis.
2	The distribution of Asaluyeh is the same across categories of VAR2.	0.000	Reject the null hypothesis.
3	The distribution of Zabol is the same across categories of VAR3.	0.314 ^a	Retain the null hypothesis.

Asymptotic significances are displayed. The significance level is 0.05.

a Exact significance is displayed for this test

Figure 2. The results of Mann–Whitney U test for indoor and outdoor dust samples in Ahvaz, Asaluyeh, and Zabol cities.

The Hg concentrations in indoor and outdoor dust from all the investigated cities were not found to be correlated, suggesting different conditions, sources, and episodic events of enhanced Hg in each city and dust sample. Nevertheless, both types of dust showed a decreasing pattern of PBM concentrations from Ahvaz to Asaluyeh and Zabol, indicating that Ahvaz dust was more significantly loaded with PBM. Comparable results were documented for the road dust in Ahvaz from different industrial, traffic, and residential sites, with mean Hg values of 0.05, 0.49, and 0.04 mg kg⁻¹ [87]. Another study on Hg levels in street dust of Ahvaz conducted by Nazarpour et al. [58] showed an average concentration of 2.53 mg kg⁻¹, ranging from 0.02 to 8.75 mg kg⁻¹. A previous study in Asaluyeh [57] showed a very similar Hg concentration (0.03 mg Kg⁻¹) from street dust samples, while to the best of our knowledge, no previous research regarding Hg was conducted in Zabol.

The reported average content of Hg in the continental crust and global surface soils is about 0.07 mg kg⁻¹, ranging from 0.03 to 0.1 mg kg⁻¹, [73,88], while highly Hg-contaminated sites generally exhibit soil concentrations of 2- to 4-orders of magnitude higher [89–91]. In general, in urban environments, the concentration of particulate mercury is highly variable due to the intervention of different anthropogenic factors. Mercury concentrations in dust samples from 60 cities in China ranged from 0.020–39.1 mg kg⁻¹, with a median value of 0.457 mg kg⁻¹ [92]. The average concentrations of mercury in dust samples from various cities throughout the world are listed in Table 2. Data on household dust Hg concentration are rather scarce in the literature. These comparisons should consider the influence of methodological differences in various studies, as well as the geological features of each region and their contribution to elemental concentrations in dust samples, apart from differences in emission sources. Regarding indoor dust, it should be noted that the characteristics of each construction, including age, elevation, renovation history, building tightness, distance from roads and industries, number of occupants, and lifestyle, may contribute to significant differences in PBM and PTE concentrations between houses at the same site [81,93–95]. In addition, different times of natural ventilation of homes by opening windows may highly differentiate the PBM levels [78]. It has been stated that PBM can also be related to household appliances and electronic products [96]. Potential indoor sources for Hg include gas-fired appliances (ovens, water heaters, furnaces), LCD screens and monitors, batteries (mainly button cell batteries), old model electrical devices with mercury switches, chest freezers, clothes dryers, clothes irons, washing machines, fluorescent bulbs, neon lights, and thermometers [97,98]. All these factors may justify the wide variation in Hg

concentration in urban environments and from one residence to another, even within the same district. In addition, the presence of Hg mine and chlor-alkali plants was identified as the main source of PBM in dust in certain cities, such as Idrija, Slovenia (20.9 mg kg^{-1} [99]), and Grenoble, France [100]. In general, the PBM concentrations of outdoor dust in the cities examined here are lower than those observed in highly polluted and industrialized megacities, such as Beijing and Nanjing. Hamedan city (~800,000 inhabitants) in west Iran also exhibited higher Hg concentrations for outdoor dust samples (Table 2).

The results of this study do not lead to a robust conclusion about the sources of Hg in the studied cities. However, it is likely that oil and gas flare burnings are associated with enhanced mercury emissions in Ahvaz and Asaluyeh, respectively. Mercury is a naturally occurring element in oil and gas and its concentration in crude oil can reach up to 10 mg kg^{-1} [101]. Ahvaz city is downwind of a supergiant oilfield, called “Ahvaz”, and it is in the vicinity of another large oilfield called “Ramin”. Several operating wells are producing crude oil from these fields, and they continuously burn the flare gas. For example, operation unit No₂ is burning 10 million cubic feet of petroleum-associated gas per day. The locations of the oilfields and major gas fields in the area are shown in Figure 3. It is inferred that the flare gases of the wells might be responsible for the elevated concentration of PBM in this city. This source factor can surely be considered along with the influence of several metal smelting plants in Ahvaz, of which the role in releasing mercury in the atmosphere cannot be overlooked.

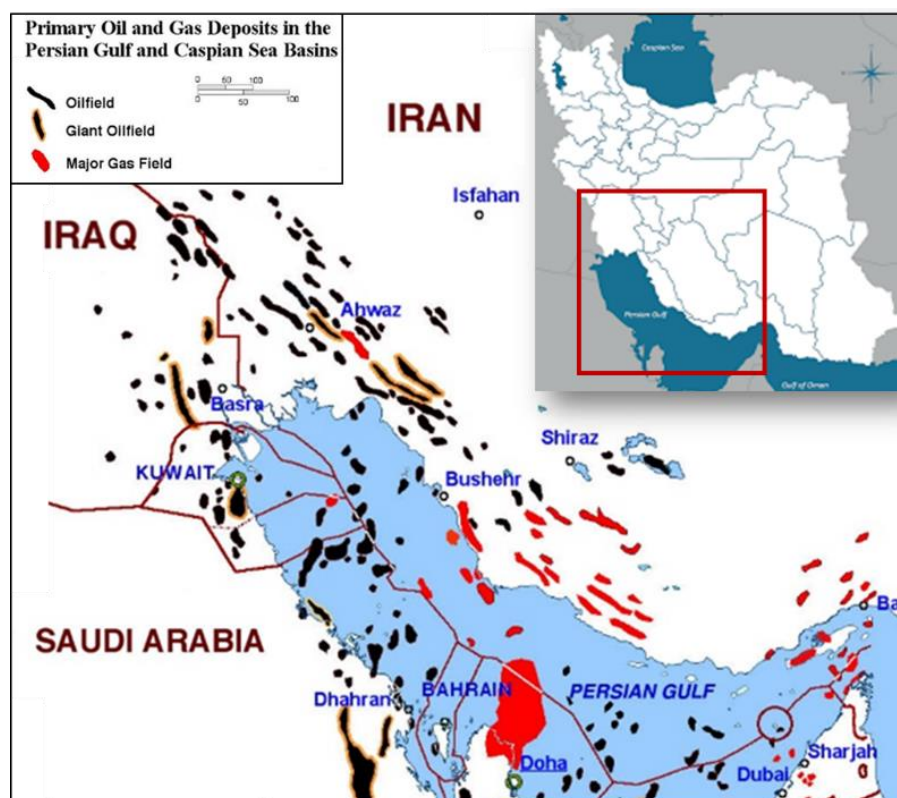


Figure 3. Distribution of oil and gas fields surrounding the cities studied in the Persian Gulf.

As mentioned above, the study area in Asaluyeh is adjacent to the South-Pars Gas-Condensate field. Hydrocarbon gases contain a lower concentration of total mercury than crude oil, and this may explain the lower concentration of PBM in Asaluyeh dust compared to Ahvaz dust. Because of the lack of a specific anthropogenic source, it is supposed that particulate-bound mercury in Zabol has a geogenic source. The normal distribution of Hg in both dust types and the insignificant difference between Hg concentrations in household and outdoor dust samples in Zabol is in agreement with this assumption.

4.2. Degree of Contamination by PBM

The contamination factor (CF) for PBM in indoor and outdoor urban dust of Ahvaz, Asaluyeh, and Zabol was calculated and illustrated in the boxplots of Figure 4.

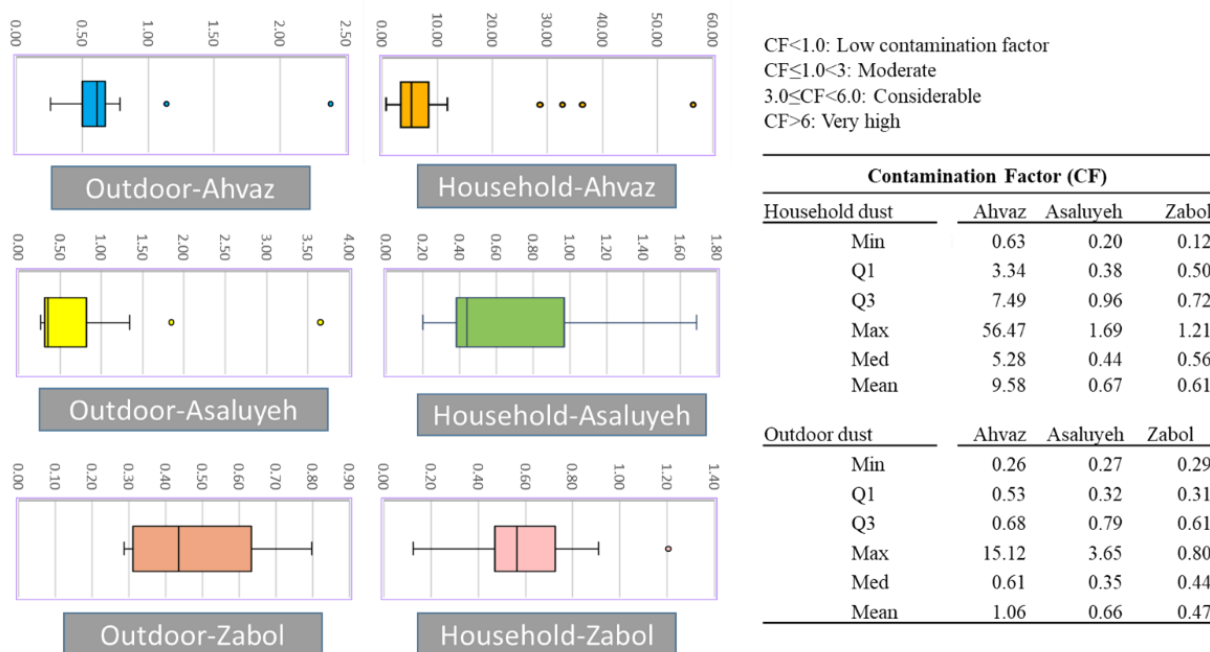


Figure 4. Box plots of contamination factor (CF) in the studied urban dusts of Ahvaz, Asaluyeh, and Zabol; the band near the middle of each box represents the median. The bottom and top of the box are the first and third quartiles, respectively. Whiskers (the vertical lines) are the 1.5 interquartile ranges of the lower and upper quartiles. Circles denote the outliers.

The highest contamination factor was observed for Hg in the indoor dust of Ahvaz, with an average CF value of 9.58. About 42% of the household Ahvaz samples exhibited CFs ranging from 6.03 to 56.47, which indicated a very high level of contamination.

The majority of the indoor dust samples in Asaluyeh (77%) were in the category of low contamination for mercury (CF < 1), and the remaining revealed moderate contamination, with CF values in the range of 1.00–1.69. The lowest contamination in indoor dust was observed for the Zabol samples, with an average CF = 0.61. This indicates that despite the intense dust storms in Zabol, contamination by PBM appears to be of relatively low concern, as opposed to other PTEs, such as Pb, Cr, Cu, and Zn, that exhibited high Enrichment Factor (EF) values [102]. A similar finding was reported for Zahedan city, in the same province as Zabol (~200 km to the south) [103].

For outdoor dust in Ahvaz, the average CF of Hg was 1.06, while for Asaluyeh and Zabol, low contamination was found for the outdoor samples, with average CF values of less than one (Figure 4). Considerable-to-high levels of Hg contamination were reported in street dust in other cities in Khuzestan province, attributed to petrochemical industries and oil refinery plants in these areas [104]. According to Mokhtarzadeh et al. [105], about 85.0% of Hg in soils of the Arvand Free Zone in Khuzestan is generated by oil products.

4.3. Non-Carcinogenic Health Risk Assessment

Based on the average daily intake of particulate-bound mercury through the ingestion, inhalation, and dermal pathways, non-cancer health risk was assessed for dwellers of Ahvaz, Asaluyeh, and Zabol cities. The results are summarized in Figure 5 and Table 3.



Figure 5. Hazard index of PBM in urban indoor and outdoor dusts of the studied cities for children and adults and the Grade (I) threshold (HI = 1.00).

Table 3. Hazard quotient (HQ) and hazard risk (HI) for PBM in urban indoor and outdoor dusts in the studied cities through three exposure routes.

Household		Adults				Children			
		HQ(ing)	HQ(inh)	HQ(drm)	HI	HQ(ing)	HQ(inh)	HQ(drm)	HI
Ahvaz	Min	3.76×10^{-7}	3.10×10^{-6}	7.51×10^{-9}	3.48×10^{-6}	3.51×10^{-6}	1.11×10^{-1}	1.76×10^{-5}	1.11×10^{-1}
	Max	3.38×10^{-5}	2.79×10^{-4}	6.75×10^{-7}	3.13×10^{-4}	3.16×10^{-4}	9.98	1.58×10^{-3}	9.98
	Med	3.16×10^{-6}	2.61×10^{-5}	6.31×10^{-8}	2.93×10^{-5}	2.95×10^{-5}	9.33×10^{-1}	1.48×10^{-4}	9.33×10^{-1}
Asaluyeh	Min	1.19×10^{-7}	9.80×10^{-7}	2.37×10^{-9}	1.10×10^{-6}	1.11×10^{-6}	3.51×10^{-1}	5.55×10^{-6}	3.51×10^{-2}
	Max	1.01×10^{-6}	8.33×10^{-6}	2.02×10^{-8}	9.36×10^{-6}	9.44×10^{-6}	2.98×10^{-1}	4.72×10^{-5}	2.98×10^{-1}
	Med	2.65×10^{-7}	2.18×10^{-6}	5.28×10^{-9}	2.45×10^{-6}	2.47×10^{-6}	7.80×10^{-2}	1.23×10^{-5}	7.80×10^{-2}
Zabol	Min	7.47×10^{-8}	6.15×10^{-7}	1.49×10^{-9}	6.91×10^{-7}	6.97×10^{-7}	2.20×10^{-2}	3.49×10^{-6}	2.20×10^{-2}
	Max	7.23×10^{-7}	5.95×10^{-6}	1.44×10^{-8}	6.69×10^{-6}	6.74×10^{-6}	2.13×10^{-1}	3.37×10^{-5}	2.13×10^{-1}
	Med	3.37×10^{-7}	2.77×10^{-6}	6.72×10^{-9}	3.11×10^{-6}	3.14×10^{-6}	9.92×10^{-2}	1.57×10^{-5}	9.92×10^{-2}
Outdoor									
Ahvaz	Min	1.55×10^{-7}	1.28×10^{-6}	3.10×10^{-9}	1.44×10^{-6}	1.45×10^{-6}	4.58×10^{-2}	7.25×10^{-6}	4.58×10^{-2}
	Max	9.06×10^{-6}	7.46×10^{-5}	1.81×10^{-7}	8.38×10^{-5}	8.46×10^{-5}	2.67	4.23×10^{-4}	2.67
	Med	3.67×10^{-7}	3.02×10^{-6}	7.32×10^{-9}	3.39×10^{-6}	3.42×10^{-6}	1.08×10^{-1}	1.71×10^{-5}	1.08×10^{-1}
Asaluyeh	Min	1.59×10^{-7}	1.31×10^{-6}	3.18×10^{-9}	1.47×10^{-6}	1.49×10^{-6}	4.70×10^{-2}	7.44×10^{-6}	4.70×10^{-2}
	Max	4.90×10^{-7}	4.04×10^{-6}	9.78×10^{-9}	4.54×10^{-6}	4.57×10^{-6}	1.44×10^{-1}	2.29×10^{-5}	1.44×10^{-1}
	Med	1.94×10^{-7}	1.6×10^{-6}	3.86×10^{-9}	1.80×10^{-6}	1.81×10^{-6}	5.71×10^{-2}	9.04×10^{-6}	5.71×10^{-2}
Zabol	Min	6.95×10^{-9}	5.72×10^{-8}	1.39×10^{-10}	6.43×10^{-8}	6.49×10^{-8}	2.05×10^{-3}	3.24×10^{-7}	2.05×10^{-3}
	Max	8.04×10^{-7}	6.62×10^{-6}	1.60×10^{-8}	7.44×10^{-6}	7.50×10^{-6}	2.37×10^{-1}	3.75×10^{-5}	2.37×10^{-1}
	Med	4.17×10^{-7}	3.44×10^{-6}	8.32×10^{-9}	3.87×10^{-6}	3.89×10^{-6}	1.23×10^{-1}	1.95×10^{-5}	1.23×10^{-1}

According to the USEPA model for non-carcinogenic health risk assessment, the average daily intake of Hg is over one order of magnitude higher in children than adults in all of the studied areas. The highest ADI value across the three routes of exposure was 8.5×10^{-6} for Ahvaz children exposed to indoor dust.

Model calculations of the hazard quotient (HQ) showed that inhalation can initiate detrimental health effects in residents of the three studied cities more than other routes of intake. In other words, HQ_{inh} was estimated as the most harmful pathway for both population groups, as also shown by other studies on the risk of exposure to mercury from urban dusts [106–108]. The trend of children > adults, as also reported in other urban areas [109–111], demonstrates that children are at higher risk of being affected by PBM due to lower body weight, their habit of playing on the ground, and the hand-to-mouth pathway [78].

As expected, the obtained HQ value was relatively higher for the inhabitants of Ahvaz city (Table 3), due to higher PBM concentrations for both indoor and outdoor dust samples. The highest likelihood of non-carcinogenic risk was found to be through the inhalation of PBM by children ($HQ_{inh} = 9.98$) and adults ($HQ_{inh} = 2.67$) in Ahvaz. Asaluyeh was the second city revealing the remarkable value of HQ_{inh} for children through indoor (2.98×10^{-1}) and outdoor dust ($1.44E \times 10^{-1}$). Absorption of Hg by inhalation showed low-to-moderate potential to cause non-carcinogenic effects in the city dwellers ($HQ < 0.1$ to $0.1 \leq HQ < 1$). As for the dermal contact pathway, the highest and the lowest hazard quotient threatening children were estimated to be in Ahvaz (1.58×10^{-3}) and Zabol (3.24×10^{-7}). HQ_{ing} was found to have the least contribution to the total non-carcinogenic health risk of Hg.

For the overall accumulative non-carcinogenic risks, the HI values ranged from 1.11×10^{-1} to 9.98 (median 9.33×10^{-1}) for indoor and from 4.58×10^{-2} to 2.67 (median 1.08×10^{-1}) for outdoor dust of Ahvaz (Table 3). The median HI value for indoor dust in Ahvaz was about 10 times higher than in other investigated cities. About 44% of the indoor dust samples taken in Ahvaz showed high levels of non-cancer health risk ($HI \geq 10$). None of the Ahvaz indoor dust samples fell in the category “no risk” or “low risk” ($HI < 0.1$ and $0.1 \leq HI < 1$, respectively) for children (Figure 5). In Asaluyeh, the HI values ranged from 3.51×10^{-2} to 2.98×10^{-1} (median 7.80×10^{-2}) for indoor and from 4.7×10^{-2} to 1.44×10^{-1} (median 5.71×10^{-2}) for outdoor dust, which is in long term exposed to children. These results indicate that young residents of Asaluyeh are at low-to-moderate levels of risk caused by PBM indoors and outdoors. The difference in Hg health risk for children between the indoor and outdoor dust samples in Zabol was negligible, as justified by the very close median HI values of 0.10 and 0.12, respectively. The health-risk estimates showed that the overall non-carcinogenic risks of Hg were within the safe allowable limit ($HI \leq 1$) for adults in all studied cities. This result is consistent with those of other studies that have shown no non-carcinogenic risks of Hg for adults [4].

The current results show that PBM in the dust of Ahvaz city has considerable potential to cause non-carcinogenic risks to young residents. Moreover, the risk associated with indoor dust is even higher. It is important to consider that simultaneous exposure to two or more PTEs may have cumulative effects on human health [112]. According to previous studies [10,113], Ahvaz soil and dust are moderate to heavily contaminated by other elements, including Cd, Cu, Pb, and Zn, which can amplify the negative health impacts of Hg on the human body. Moreover, the current estimation has taken into account only one urban medium (dust). Hg contamination and health impacts can be introduced and magnified in the human body via other compartments of soil, water, and food. A previous study in Ahvaz showed that the inhalation cancer risks and HIs of Pb, Cr, and Ni were lower than the threshold limits [63].

Some alarming health risks of up to moderate levels were observed for children in Asaluyeh and Zabol cities. It is worth mentioning that even though Hg does not seem to represent a non-carcinogenic risk for adults, the population of the studied cities is predicted to be at morbidity and mortality risk due to the long-term exposure to fine particulate matter

generated as a consequence of intense dust storms over their adjacent arid and semi-arid regions, as previous studies in both sites have shown [57,69]. Especially in Zabol, a recent study [55] revealed very high health risks related to PTEs (Mn, Zn, Pb, As, Cu, Cd, Cr, Co, Ni) in TSP and PM_{2.5} airborne dust samples. More specifically, the non-carcinogenic risks for individual PTEs were above the safe limit (HI > 1) for inhalation and dermal contact in both population groups, as well as ingestion for children. Furthermore, high cancer risks were estimated in Zabol for the ingestion pathway ($1.2\text{--}2.8 \times 10^{-4}$), while cancer risks above the safe limit of 10^{-4} for inhalation and dermal contact were found in adults. Similar to the current results, inhalation was the pathway with the highest non-carcinogenic risk in Zabol.

Dust emissions and their related health impacts are a topic of worldwide concern [114]. However, the health risk assessment should be critically considered in view of the underlying assumptions included in the USEPA model [75]. Parameters, such as body weight, exposure duration, frequency, and average time may differentiate between population groups in different countries or between people living and working in rural or urban environments. These assumptions may significantly influence the estimates of actual health risk on children and adults, and several countries have different regulation limits of PTEs, resulting in different risk assessments [115]. Moreover, only total Hg data are available in this study, which may add further uncertainty to the risk estimates, since Hg species may be very different in bioavailability and toxicity, and therefore, have different consequences for the health risk.

5. Future Perspectives

This research raises several questions that need further investigation. The anthropogenic emissions of Hg can lead to a general increase in the content of this element locally, regionally, and globally. Hence, detailed geochemical studies on mercury in soil and airborne dust samples over Iranian cities, and in particular, in the critical oil and gas producing urban areas in the south and southwest of the country, are needed. Further studies should consider the emission characteristics of all forms of Hg to better understand the possible health risks associated with different species and their role in the transport and deposition of PBM. More work is recommended on source identification and spatial distribution patterns of mercury, especially in highly polluted and industrialized cities like Ahvaz. Analyses of PBM with the wind direction, and based on particle-size classification and the binding mechanisms between Hg and dust particles are also suggested. In response to the increasing concerns regarding identification of dust emissions in the Middle East, as a consequence of climate change, decrease in precipitation, increase in temperature, and desertification [116], investigating the cumulative effects of joint exposure to PBM and other PTEs in urban dust may provide a more realistic perspective on the likelihood and degree of human health impacts.

6. Conclusions

This study provided for the first time data on the concentration of particulate-bound mercury in indoor and outdoor dust of three Iranian cities, Ahvaz, Asaluyeh, and Zabol. Even though PBM in the investigated cities was not found in concentrations as high as in some heavily polluted megacities, such as Beijing, it still represents a potential health risk for residents. The Hg concentration in the analyzed dust samples appeared to be the highest in Ahvaz, followed by Asaluyeh and Zabol. This trend showed a correlation with the stage of industrial development and the presence of oil and gas-related activities, which prevail in Ahvaz. The comparison of Hg concentrations in outdoor vs. indoor dust in Ahvaz and Asaluyeh were found to be indoor dust > outdoor dust, whereas this difference was not observed in Zabol. This evidence, along with the normal distribution of Hg across all samples and the absence of any specific source of anthropogenic Hg emissions in Zabol, suggests a geogenic origin of the metal. According to the USEPA model for health risk assessment, the inhalation pathway for PBM was recognized as the main route of exposure

posing a potential health risk for people in the studied cities. The population of children in Ahvaz is expected to be at a high level of no-carcinogenic risk caused by Hg in household dust. In contrast, the potential occurrence of chronic non-carcinogenic health problems in children of Asaluyeh and Zabol was low to moderate. Adults showed a similar trend of Hg hazard index; however, they are less prone to be affected by PBM in indoor and outdoor dust in any city.

Author Contributions: Conceptualization, R.D.B. and M.T.; methodology, R.D.B., M.T., and R.A.; formal analysis, R.D.B., M.T., and A.E.-S.; data curation, R.D.B., M.T., and R.A.; writing—original draft preparation, R.D.B.; writing—review and editing, R.D.B., M.T., and D.G.K.; supervision, D.G.K. All authors have read and agreed to the published version of the manuscript.

Funding: This research received no external funding.

Institutional Review Board Statement: Not applicable.

Informed Consent Statement: Not applicable.

Data Availability Statement: The data can be available upon request.

Acknowledgments: This article was supported by the University of Zabol (Iran) with grant code (UOZ-GR-9618-91). We are thankful to all individuals who kindly helped in indoor dust sampling.

Conflicts of Interest: The authors declare no conflict of interest.

References

1. Manalis, N.; Grivas, G.; Protonotarios, V.; Moutsatsou, A.; Samara, C.; Chaloulakou, A. Toxic metal content of particulate matter (PM₁₀), within the Greater Area of Athens. *Chemosphere* **2005**, *60*, 557–566. [[CrossRef](#)]
2. Mihankhah, T.; Saeedi, M.; Karbassi, A. A comparative study of elemental pollution and health risk assessment in urban dust of different land-uses in Tehran's urban area. *Chemosphere* **2020**, *241*, 124984. [[CrossRef](#)] [[PubMed](#)]
3. Aguilera, A.; Bautista, F.; Gutiérrez-Ruiz, M.; Cenicerós-Gómez, A.E.; Cejudo, R.; Goguitchaichvili, A. Heavy metal pollution of street dust in the largest city of Mexico, sources and health risk assessment. *Environ. Monit. Assess.* **2021**, *193*, 1–16. [[CrossRef](#)]
4. Hu, X.; Zhang, Y.; Luo, J.; Wang, T.; Lian, H.; Ding, Z. Bioaccessibility and health risk of arsenic, mercury and other metals in urban street dusts from a mega-city, Nanjing, China. *Environ. Pollut.* **2011**, *159*, 1215–1221. [[CrossRef](#)]
5. Marx, S.K.; Kamber, B.S.; McGowan, H.A. Scavenging of atmospheric trace metal pollutants by mineral dusts: Inter-regional transport of Australian trace metal pollution to New Zealand. *Atmos. Environ.* **2008**, *42*, 2460–2478. [[CrossRef](#)]
6. Dehghani, S.; Moore, F.; Vasiluk, L.; Hale, B.A. The geochemical fingerprinting of geogenic particles in road deposited dust from Tehran metropolis, Iran: Implications for provenance tracking. *J. Geochem. Explor.* **2018**, *190*, 411–423. [[CrossRef](#)]
7. Ali, M.U.; Liu, G.; Yousaf, B.; Ullah, H.; Abbas, Q.; Munir, M.A.M. A systematic review on global pollution status of particulate matter-associated potential toxic elements and health perspectives in urban environment. *Environ. Geochem. Health* **2019**, *41*, 1131–1162. [[CrossRef](#)]
8. Galindo, N.; Yubero, E.; Nicolás, J.; Varea, M.; Crespo, J. Characterization of metals in PM₁ and PM₁₀ and health risk evaluation at an urban site in the western Mediterranean. *Chemosphere* **2018**, *201*, 243–250. [[CrossRef](#)]
9. Shahsavani, A.; Tobías, A.; Querol, X.; Stafoggia, M.; Abdolshahnejad, M.; Mayvaneh, F.; Guo, Y.; Hadei, M.; Hashemi, S.S.; Khosravi, A. Short-term effects of particulate matter during desert and non-desert dust days on mortality in Iran. *Environ. Int.* **2020**, *134*, 105299. [[CrossRef](#)]
10. Tashakor, M.; Modabberi, S.; Argyraki, A. Assessing the contamination level, sources and risk of potentially toxic elements in urban soil and dust of Iranian cities using secondary data of published literature. *Environ. Geochem. Health* **2022**, *44*, 645–675. [[CrossRef](#)]
11. Adimalla, N. Heavy metals pollution assessment and its associated human health risk evaluation of urban soils from Indian cities: A review. *Environ. Geochem. Health* **2020**, *42*, 173–190. [[CrossRef](#)]
12. Morera-Gómez, Y.; Alonso-Hernández, C.M.; Santamaría, J.M.; Elustondo, D.; Lasheras, E.; Widory, D. Levels, spatial distribution, risk assessment, and sources of environmental contamination vectored by road dust in Cienfuegos (Cuba) revealed by chemical and C and N stable isotope compositions. *Environ. Sci. Pollut. Res.* **2020**, *27*, 2184–2196. [[CrossRef](#)]
13. Golia, E.; Tsiropoulos, G.; Füleky, G.; Floras, S.; Vleioras, S. Pollution assessment of potentially toxic elements in soils of different taxonomy orders in central Greece. *Environ. Monit. Assess.* **2019**, *191*, 106. [[CrossRef](#)]
14. Parlak, M.; Tunçay, T.; Botsou, F. Heavy Metals in Soil and Sand from Playgrounds of Çanakkale City (Turkey), and Related Health Risks for Children. *Sustainability* **2022**, *14*, 1145. [[CrossRef](#)]
15. Hu, X.; Zhang, Y.; Ding, Z.; Wang, T.; Lian, H.; Sun, Y.; Wu, J. Bioaccessibility and health risk of arsenic and heavy metals (Cd, Co, Cr, Cu, Ni, Pb, Zn and Mn) in TSP and PM_{2.5} in Nanjing, China. *Atmos. Environ.* **2012**, *57*, 146–152. [[CrossRef](#)]

16. Cao, S.; Duan, X.; Zhao, X.; Ma, J.; Dong, T.; Huang, N.; Sun, C.; He, B.; Wei, F. Health risks from the exposure of children to As, Se, Pb and other heavy metals near the largest coking plant in China. *Sci. Total Environ.* **2014**, *472*, 1001–1009. [[CrossRef](#)]
17. Nazarpour, A.; Watts, M.J.; Madhani, A.; Elahi, S. Source, spatial distribution and pollution assessment of Pb, Zn, Cu, and Pb, isotopes in urban soils of Ahvaz City, a semi-arid metropolis in southwest Iran. *Sci. Rep.* **2019**, *9*, 5349. [[CrossRef](#)]
18. Wright, L.P.; Zhang, L.; Cheng, I.; Aherne, J.; Wentworth, G.R. Impacts and effects indicators of atmospheric deposition of major pollutants to various ecosystems—A review. *Aerosol Air Qual. Res.* **2018**, *18*, 1953–1992. [[CrossRef](#)]
19. Guo, J.; Ram, K.; Tripathee, L.; Kang, S.; Huang, J.; Chen, P.; Ghimire, P.S. Study on Mercury in PM10 at an Urban Site in the Central Indo-Gangetic Plain: Seasonal Variability and Influencing Factors. *Aerosol Air Qual. Res.* **2020**, *20*, 2729–2740. [[CrossRef](#)]
20. Chen, X.; Xia, X.; Wu, S.; Wang, F.; Guo, X. Mercury in urban soils with various types of land use in Beijing, China. *Environ. Pollut.* **2010**, *158*, 48–54. [[CrossRef](#)]
21. Fang, F.; Wang, Q.; Li, J. Urban environmental mercury in Changchun, a metropolitan city in Northeastern China: Source, cycle, and fate. *Sci. Total Environ.* **2004**, *330*, 159–170. [[CrossRef](#)] [[PubMed](#)]
22. Brown, A.D.; Yalala, B.; Cukrowska, E.; Godoi, R.H.; Potgieter-Vermaak, S. A scoping study of component-specific toxicity of mercury in urban road dusts from three international locations. *Environ. Geochem. Health* **2020**, *42*, 1127–1139. [[CrossRef](#)] [[PubMed](#)]
23. Liu, R.; Wang, Q.; Lu, X.; Fang, F.; Wang, Y. Distribution and speciation of mercury in the peat bog of Xiaoxing'an Mountain, northeastern China. *Environ. Pollut.* **2003**, *124*, 39–46. [[CrossRef](#)]
24. Pacyna, E.G.; Pacyna, J.; Sundseth, K.; Munthe, J.; Kindbom, K.; Wilson, S.; Steenhuisen, F.; Maxson, P. Global emission of mercury to the atmosphere from anthropogenic sources in 2005 and projections to 2020. *Atmos. Environ.* **2010**, *44*, 2487–2499. [[CrossRef](#)]
25. Bindler, R. Estimating the natural background atmospheric deposition rate of mercury utilizing ombrotrophic bogs in southern Sweden. *Environ. Sci. Technol.* **2003**, *37*, 40–46. [[CrossRef](#)]
26. Arctic Monitoring and Assessment Programme (AMAP); United Nations Environment Programme (UNEP). *Technical Background Report to the Global Atmospheric Mercury Assessment*; Arctic Monitoring and Assessment Programme: Oslo, Norway; UNEP Chemicals Branch: Nairobi, Kenya, 2008.
27. Kelepertzis, E.; Argyraki, A. Mercury in the urban topsoil of Athens, Greece. *Sustainability* **2015**, *7*, 4049–4062. [[CrossRef](#)]
28. Chung, S.; Chon, H.-T. Assessment of the level of mercury contamination from some anthropogenic sources in Ulaanbaatar, Mongolia. *J. Geochem. Explor.* **2014**, *147*, 237–244. [[CrossRef](#)]
29. Driscoll, C.T.; Mason, R.P.; Chan, H.M.; Jacob, D.J.; Pirrone, N. Mercury as a global pollutant: Sources, pathways, and effects. *Environ. Sci. Technol.* **2013**, *47*, 4967–4983. [[CrossRef](#)]
30. Rodrigues, S.; Pereira, M.; Duarte, A.; Ajmone-Marsan, F.; Davidson, C.; Grčman, H.; Hossack, I.; Hursthouse, A.; Ljung, K.; Martini, C. Mercury in urban soils: A comparison of local spatial variability in six European cities. *Sci. Total Environ.* **2006**, *368*, 926–936. [[CrossRef](#)]
31. Yu, G.; Qin, X.; Xu, J.; Zhou, Q.; Wang, B.; Huang, K.; Deng, C. Characteristics of particulate-bound mercury at typical sites situated on dust transport paths in China. *Sci. Total Environ.* **2019**, *648*, 1151–1160. [[CrossRef](#)]
32. Lindberg, S.a.; Stratton, W. Atmospheric mercury speciation: Concentrations and behavior of reactive gaseous mercury in ambient air. *Environ. Sci. Technol.* **1998**, *32*, 49–57. [[CrossRef](#)]
33. Schleicher, N.; Schäfer, J.; Blanc, G.; Chen, Y.; Chai, F.; Cen, K.; Norra, S. Atmospheric particulate mercury in the megacity Beijing: Spatio-temporal variations and source apportionment. *Atmos. Environ.* **2015**, *109*, 251–261. [[CrossRef](#)]
34. Guo, J.; Kang, S.; Huang, J.; Zhang, Q.; Rupakheti, M.; Sun, S.; Tripathee, L.; Rupakheti, D.; Panday, A.K.; Sillanpää, M. Characterizations of atmospheric particulate-bound mercury in the Kathmandu Valley of Nepal, South Asia. *Sci. Total Environ.* **2017**, *579*, 1240–1248. [[CrossRef](#)]
35. Morel, F.M.; Kraepiel, A.M.; Amyot, M. The chemical cycle and bioaccumulation of mercury. *Annu. Rev. Ecol. Syst.* **1998**, *29*, 543–566. [[CrossRef](#)]
36. Shannon, J.D.; Voldner, E.C. Modeling atmospheric concentrations of mercury and deposition to the Great Lakes. *Atmos. Environ.* **1995**, *29*, 1649–1661. [[CrossRef](#)]
37. Sun, J.; Shen, Z.; Zhang, L.; Lei, Y.; Gong, X.; Zhang, Q.; Zhang, T.; Xu, H.; Cui, S.; Wang, Q. Chemical source profiles of urban fugitive dust PM_{2.5} samples from 21 cities across China. *Sci. Total Environ.* **2019**, *649*, 1045–1053. [[CrossRef](#)]
38. Aslam, M.W.; Ali, W.; Meng, B.; Abrar, M.M.; Lu, B.; Qin, C.; Zhao, L.; Feng, X. Mercury contamination status of rice cropping system in Pakistan and associated health risks. *Environ. Pollut.* **2020**, *263*, 114625. [[CrossRef](#)]
39. Nie, X.; Mao, H.; Li, P.; Li, T.; Zhou, J.; Wu, Y.; Yang, M.; Zhen, J.; Wang, X.; Wang, Y. Total gaseous mercury in a coastal city (Qingdao, China): Influence of sea-land breeze and regional transport. *Atmos. Environ.* **2020**, *235*, 117633. [[CrossRef](#)]
40. Coufalík, P.; Zvěřina, O.; Mikuška, P.; Komárek, J. Seasonal variability of mercury contents in street dust in Brno, Czech Republic. *Bull. Environ. Contam. Toxicol.* **2014**, *93*, 503–508. [[CrossRef](#)]
41. Clarkson, T.W.; Magos, L.; Myers, G.J. The toxicology of mercury—Current exposures and clinical manifestations. *N. Engl. J. Med.* **2003**, *349*, 1731–1737. [[CrossRef](#)]
42. Ordóñez, A.; Álvarez, R.; De Miguel, E.; Charlesworth, S. Spatial and temporal variations of trace element distribution in soils and street dust of an industrial town in NW Spain: 15 years of study. *Sci. Total Environ.* **2015**, *524*, 93–103. [[CrossRef](#)] [[PubMed](#)]
43. Sondreal, E.A.; Benson, S.A.; Pavlish, J.H.; Ralston, N.V. An overview of air quality III: Mercury, trace elements, and particulate matter. *Fuel Processing Technol.* **2004**, *85*, 425–440. [[CrossRef](#)]

44. Lu, X.; Li, L.Y.; Wang, L.; Lei, K.; Huang, J.; Zhai, Y. Contamination assessment of mercury and arsenic in roadway dust from Baoji, China. *Atmos. Environ.* **2009**, *43*, 2489–2496. [[CrossRef](#)]
45. Charlesworth, S.; De Miguel, E.; Ordóñez, A. A review of the distribution of particulate trace elements in urban terrestrial environments and its application to considerations of risk. *Environ. Geochem. Health* **2011**, *33*, 103–123. [[CrossRef](#)]
46. Massey, D.D.; Kulshrestha, A.; Taneja, A. Particulate matter concentrations and their related metal toxicity in rural residential environment of semi-arid region of India. *Atmos. Environ.* **2013**, *67*, 278–286. [[CrossRef](#)]
47. Carpi, A.; Chen, Y.-f. Gaseous elemental mercury as an indoor air pollutant. *Environ. Sci. Technol.* **2001**, *35*, 4170–4173. [[CrossRef](#)]
48. Koehler, K.; Good, N.; Wilson, A.; Mölter, A.; Moore, B.F.; Carpenter, T.; Peel, J.L.; Volckens, J. The Fort Collins commuter study: Variability in personal exposure to air pollutants by microenvironment. *Indoor Air* **2019**, *29*, 231–241. [[CrossRef](#)]
49. Huang, M.; Wang, W.; Chan, C.Y.; Cheung, K.C.; Man, Y.B.; Wang, X.; Wong, M.H. Contamination and risk assessment (based on bioaccessibility via ingestion and inhalation) of metal (loid) s in outdoor and indoor particles from urban centers of Guangzhou, China. *Sci. Total Environ.* **2014**, *479*, 117–124. [[CrossRef](#)]
50. Ali, M.U.; Liu, G.; Yousaf, B.; Abbas, Q.; Ullah, H.; Munir, M.A.M.; Zhang, H. Compositional characteristics of black-carbon and nanoparticles in air-conditioner dust from an inhabitable industrial metropolis. *J. Clean. Prod.* **2018**, *180*, 34–42. [[CrossRef](#)]
51. Verdenelli, M.; Cecchini, C.; Orpiani, C.; Dadea, G.; Cresci, A. Efficacy of antimicrobial filter treatments on microbial colonization of air panel filters. *J. Appl. Microbiol.* **2003**, *94*, 9–15. [[CrossRef](#)]
52. Nourmoradi, H.; Khaniabadi, Y.O.; Goudarzi, G.; Daryanoosh, S.M.; Khoshgoftar, M.; Omid, F.; Armin, H. Air quality and health risks associated with exposure to particulate matter: A cross-sectional study in Khorramabad, Iran. *Health Scope* **2016**, *5*, e31766. [[CrossRef](#)]
53. Norouzi, S.; Khademi, H.; Ayoubi, S.; Cano, A.F.; Acosta, J.A. Seasonal and spatial variations in dust deposition rate and concentrations of dust-borne heavy metals, a case study from Isfahan, central Iran. *Atmos. Pollut. Res.* **2017**, *8*, 686–699. [[CrossRef](#)]
54. Moghtaderi, T.; Aminiyan, M.M.; Alamdar, R.; Moghtaderi, M. Index-based evaluation of pollution characteristics and health risk of potentially toxic metals in schools dust of Shiraz megacity, SW Iran. *Hum. Ecol. Risk Assess. Int. J.* **2019**, *25*, 410–437. [[CrossRef](#)]
55. Dahmardeh Behrooz, R.; Kaskaoutis, D.; Grivas, G.; Mihalopoulos, N. Human health risk assessment for toxic elements in the extreme ambient dust conditions observed in Sistan, Iran. *Chemosphere* **2021**, *262*, 127835. [[CrossRef](#)]
56. Modabberi, S.; Tashakor, M.; Soltani, N.S.; Hursthouse, A.S. Potentially toxic elements in urban soils: Source apportionment and contamination assessment. *Environ. Monit. Assess.* **2018**, *190*, 715. [[CrossRef](#)]
57. Abbasi, S.; Keshavarzi, B.; Moore, F.; Mahmoudi, M.R. Fractionation, source identification and risk assessment of potentially toxic elements in street dust of the most important center for petrochemical products, Asaluyeh County, Iran. *Environ. Earth Sci.* **2018**, *77*, 673. [[CrossRef](#)]
58. Nazarpour, A.; Ghanavati, N.; Watts, M.J. Spatial distribution and human health risk assessment of mercury in street dust resulting from various land-use in Ahvaz, Iran. *Environ. Geochem. Health* **2018**, *40*, 693–704. [[CrossRef](#)]
59. Javadian, M.; Behrangi, A.; Sorooshian, A. Impact of drought on dust storms: Case study over Southwest Iran. *Environ. Res. Lett.* **2019**, *14*, 124029. [[CrossRef](#)]
60. Salmabadi, H.; Khalidy, R.; Saeedi, M. Transport routes and potential source regions of the Middle Eastern dust over Ahvaz during 2005–2017. *Atmos. Res.* **2020**, *241*, 104947. [[CrossRef](#)]
61. Hamzeh, N.H.; Karami, S.; Kaskaoutis, D.G.; Tegen, I.; Moradi, M.; Opp, C. Atmospheric dynamics and numerical simulations of six frontal dust storms in the Middle East region. *Atmosphere* **2021**, *12*, 125. [[CrossRef](#)]
62. Maleki, H.; Sorooshian, A.; Goudarzi, G.; Nikfal, A.; Baneshi, M.M. Temporal profile of PM10 and associated health effects in one of the most polluted cities of the world (Ahvaz, Iran) between 2009 and 2014. *Aeolian Res.* **2016**, *22*, 135–140. [[CrossRef](#)]
63. Goudarzi, G.; Alavi, N.; Geravandi, S.; Idani, E.; Behrooz, H.R.A.; Babaei, A.A.; Alamdari, F.A.; Dobaradaran, S.; Farhadi, M.; Mohammadi, M.J. Health risk assessment on human exposed to heavy metals in the ambient air PM10 in Ahvaz, southwest Iran. *Int. J. Biometeorol.* **2018**, *62*, 1075–1083. [[CrossRef](#)]
64. MalAmiri, N.; Rashki, A.; Hosseinzadeh, S.R.; Kaskaoutis, D. Mineralogical, geochemical, and textural characteristics of soil and airborne samples during dust storms in Khuzestan, southwest Iran. *Chemosphere* **2022**, *286*, 131879. [[CrossRef](#)]
65. Hamzeh, N.H.; Kaskaoutis, D.G.; Rashki, A.; Mohammadpour, K. Long-Term Variability of Dust Events in Southwestern Iran and Its Relationship with the Drought. *Atmosphere* **2021**, *12*, 1350. [[CrossRef](#)]
66. Miri, A.; Moghaddamnia, A.; Pahlavanravi, A.; Panjehkeh, N. Dust storm frequency after the 1999 drought in the Sistan region, Iran. *Clim. Res.* **2010**, *41*, 83–90. [[CrossRef](#)]
67. Rashki, A.; Kaskaoutis, D.; Goudie, A.S.; Kahn, R. Dryness of ephemeral lakes and consequences for dust activity: The case of the Hamoun drainage basin, southeastern Iran. *Sci. Total Environ.* **2013**, *463*, 552–564. [[CrossRef](#)]
68. Hamidianpour, M.; Jahanshahi, S.M.A.; Kaskaoutis, D.G.; Rashki, A.; Nastos, P.G. Climatology of the Sistan Levant wind: Atmospheric dynamics driving its onset, duration and withdrawal. *Atmos. Res.* **2021**, *260*, 105711. [[CrossRef](#)]
69. Javan, S.; Rahdar, S.; Miri, M.; Djahed, B.; Kazemian, H.; Fakhri, Y.; Eslami, H.; Fallahzadeh, R.A.; Gholizadeh, A.; Taghavi, M. Modeling of the PM10 pollutant health effects in a semi-arid area: A case study in Zabol, Iran. *Modeling Earth Syst. Environ.* **2021**, *7*, 455–463. [[CrossRef](#)]
70. Rashki, A.; Middleton, N.J.; Goudie, A.S. Dust storms in Iran—Distribution, causes, frequencies and impacts. *Aeolian Res.* **2021**, *48*, 100655. [[CrossRef](#)]

71. Del Rio-Salas, R.; Ruiz, J.; De la O-Villanueva, M.; Valencia-Moreno, M.; Moreno-Rodríguez, V.; Gómez-Alvarez, A.; Grijalva, T.; Mendivil, H.; Paz-Moreno, F.; Meza-Figueroa, D. Tracing geogenic and anthropogenic sources in urban dusts: Insights from lead isotopes. *Atmos. Environ.* **2012**, *60*, 202–210. [[CrossRef](#)]
72. Loska, K.; Wiechula, D.; Korus, I. Metal contamination of farming soils affected by industry. *Environ. Int.* **2004**, *30*, 159–165. [[CrossRef](#)]
73. Kabata-Pendias, A. *Trace Elements in Soils and Plants*, 4th ed.; CRS Press: Boca Raton, FL, USA, 2011.
74. Abraham, G.; Parker, R. Assessment of heavy metal enrichment factors and the degree of contamination in marine sediments from Tamaki Estuary, Auckland, New Zealand. *Environ. Monit. Assess.* **2008**, *136*, 227–238. [[CrossRef](#)] [[PubMed](#)]
75. The United States Environmental Protection Agency (USEPA). *Supplemental Guidance for Developing Soil Screening Levels for Superfund Sites*; Office of Emergency and Remedial Response, the United States Environmental Protection Agency: Washington, DC, USA, 2002.
76. Liu, E.; Yan, T.; Birch, G.; Zhu, Y. Pollution and health risk of potentially toxic metals in urban road dust in Nanjing, a mega-city of China. *Sci. Total Environ.* **2014**, *476*, 522–531. [[CrossRef](#)] [[PubMed](#)]
77. Li, H.-H.; Chen, L.-J.; Yu, L.; Guo, Z.-B.; Shan, C.-Q.; Lin, J.-Q.; Gu, Y.-G.; Yang, Z.-B.; Yang, Y.-X.; Shao, J.-R. Pollution characteristics and risk assessment of human exposure to oral bioaccessibility of heavy metals via urban street dusts from different functional areas in Chengdu, China. *Sci. Total Environ.* **2017**, *586*, 1076–1084. [[CrossRef](#)]
78. Kurt-Karakus, P.B. Determination of heavy metals in indoor dust from Istanbul, Turkey: Estimation of the health risk. *Environ. Int.* **2012**, *50*, 47–55. [[CrossRef](#)]
79. Zhang, Y.; Ji, X.; Ku, T.; Li, G.; Sang, N. Heavy metals bound to fine particulate matter from northern China induce season-dependent health risks: A study based on myocardial toxicity. *Environ. Pollut.* **2016**, *216*, 380–390. [[CrossRef](#)]
80. Xinmin, Z.; Kunli, L.; Xinzhang, S.; Jian'an, T.; Yilun, L. Mercury in the topsoil and dust of Beijing City. *Sci. Total Environ.* **2006**, *368*, 713–722. [[CrossRef](#)]
81. Ferreira-Baptista, L.; De Miguel, E. Geochemistry and risk assessment of street dust in Luanda, Angola: A tropical urban environment. *Atmos. Environ.* **2005**, *39*, 4501–4512. [[CrossRef](#)]
82. Christoforidis, A.; Stamatis, N. Heavy metal contamination in street dust and roadside soil along the major national road in Kavala's region, Greece. *Geoderma* **2009**, *151*, 257–263. [[CrossRef](#)]
83. Sahakyan, L.; Tepanosyan, G.; Maghakyan, N.; Kafyan, M.; Melkonyan, G.; Saghatlyan, A. Contamination levels and human health risk assessment of mercury in dust and soils of the urban environment, Vanadzor, Armenia. *Atmos. Pollut. Res.* **2019**, *10*, 808–816. [[CrossRef](#)]
84. Nedić, A.B.; Pucarević, M.; Ninkov, J.; Stojić, N.S.; Milić, D. Mercury content and distribution in household dust and soil in the town of Šid. *Zb. Matice Srp. Za Prir. Nauk.* **2019**, *137*, 33–41. [[CrossRef](#)]
85. Rasmussen, P.; Subramanian, K.; Jessiman, B. A multi-element profile of house dust in relation to exterior dust and soils in the city of Ottawa, Canada. *Sci. Total Environ.* **2001**, *267*, 125–140. [[CrossRef](#)]
86. Bao, L.; Wang, S.; Sun, H.; Huang, W.; Wang, G.; Nan, Z. Assessment of source and health risk of metal (loid) s in indoor/outdoor dust of university dormitory in Lanzhou City, China. *Environ. Sci. Pollut. Res.* **2019**, *26*, 32333–32344. [[CrossRef](#)]
87. Najmeddin, A.; Keshavarzi, B.; Moore, F.; Lahijan-zadeh, A. Source apportionment and health risk assessment of potentially toxic elements in road dust from urban industrial areas of Ahvaz megacity, Iran. *Environ. Geochem. Health* **2018**, *40*, 1187–1208. [[CrossRef](#)]
88. Reimann, C.; De Caritat, P. *Chemical Elements in the Environment: Factsheets for the Geochemist and Environmental Scientist*; Springer Science & Business Media: Berlin/Heidelberg, Germany, 2012.
89. Wang, J.; Feng, X.; Anderson, C.W.; Xing, Y.; Shang, L. Remediation of mercury contaminated sites—A review. *J. Hazard. Mater.* **2012**, *221*, 1–18. [[CrossRef](#)]
90. Li, S.; Jia, Z. Heavy metals in soils from a representative rapidly developing megacity (SW China): Levels, source identification and apportionment. *Catena* **2018**, *163*, 414–423. [[CrossRef](#)]
91. Gworek, B.; Dmuchowski, W.; Baczevska-Dąbrowska, A.H. Mercury in the terrestrial environment: A review. *Environ. Sci. Eur.* **2020**, *32*, 128. [[CrossRef](#)]
92. Sun, G.; Feng, X.; Yang, C.; Zhang, L.; Yin, R.; Li, Z.; Bi, X.; Wu, Y. Levels, sources, isotope signatures, and health risks of mercury in street dust across China. *J. Hazard. Mater.* **2020**, *392*, 122276. [[CrossRef](#)]
93. Grivas, G.; Cheristanidis, S.; Chaloulakou, A.; Koutrakis, P.; Mihalopoulos, N. Elemental composition and source apportionment of fine and coarse particles at traffic and urban background locations in Athens, Greece. *Aerosol Air Qual. Res.* **2018**, *18*, 1642–1659. [[CrossRef](#)]
94. Shrestha, P.M.; Humphrey, J.L.; Carlton, E.J.; Adgate, J.L.; Barton, K.E.; Root, E.D.; Miller, S.L. Impact of outdoor air pollution on indoor air quality in low-income homes during wildfire seasons. *Int. J. Environ. Res. Public Health* **2019**, *16*, 3535. [[CrossRef](#)]
95. Tian, L.; Zhang, G.; Lin, Y.; Yu, J.; Zhou, J.; Zhang, Q. Mathematical model of particle penetration through smooth/rough building envelop leakages. *Build. Environ.* **2009**, *44*, 1144–1149. [[CrossRef](#)]
96. Turner, A.; Lewis, M. Lead and other heavy metals in soils impacted by exterior legacy paint in residential areas of south west England. *Sci. Total Environ.* **2018**, *619*, 1206–1213. [[CrossRef](#)]
97. Levesque, C.; Rasmussen, P.E. Determination of Total Mercury and Carbon in a National Baseline Study of Urban House Dust. *Geosciences* **2022**, *12*, 52. [[CrossRef](#)]

98. Cao, S.; Chen, X.; Zhang, L.; Xing, X.; Wen, D.; Wang, B.; Qin, N.; Wei, F.; Duan, X. Quantificational exposure, sources, and health risks posed by heavy metals in indoor and outdoor household dust in a typical smelting area in China. *Indoor Air* **2020**, *30*, 872–884. [[CrossRef](#)]
99. Gosar, M.; Šajn, R.; Biester, H. Binding of mercury in soils and attic dust in the Idrija mercury mine area (Slovenia). *Sci. Total Environ.* **2006**, *369*, 150–162. [[CrossRef](#)] [[PubMed](#)]
100. Grangeon, S.; Guédron, S.; Asta, J.; Sarret, G.; Charlet, L. Lichen and soil as indicators of an atmospheric mercury contamination in the vicinity of a chlor-alkali plant (Grenoble, France). *Ecol. Indic.* **2012**, *13*, 178–183. [[CrossRef](#)]
101. Wilhelm, S.M.; Bloom, N. Mercury in petroleum. *Fuel Processing Technol.* **2000**, *63*, 1–27. [[CrossRef](#)]
102. Dahmardeh Behrooz, R.; Esmaili-Sari, A.; Bahramifar, N.; Kaskaoutis, D.; Saeb, K.; Rajaei, F. Trace-element concentrations and water-soluble ions in size-segregated dust-borne and soil samples in Sistan, southeast Iran. *Aeolian Res.* **2017**, *25*, 87–105. [[CrossRef](#)]
103. Mehrizi, E.; Biglari, H.; Amiri, R.; Baneshi, M.; Mobini, M.; Ebrahimzadeh, G.; Zarei, A.; Naroioie, M.R. Determine the important heavy metals in air dust of zahedan, Iran. *Pollut. Res.* **2017**, *36*, 474–480.
104. Naraki, H.; Keshavarzi, B.; Zarei, M.; Moore, F.; Abbasi, S.; Kelly, F.J.; Dominguez, A.O.; Jaafarzadeh, N. Urban street dust in the Middle East oldest oil refinery zone: Oxidative potential, source apportionment and health risk assessment of potentially toxic elements. *Chemosphere* **2021**, *268*, 128825. [[CrossRef](#)]
105. Mokhtarzadeh, Z.; Keshavarzi, B.; Moore, F.; Marsan, F.A.; Padoan, E. Potentially toxic elements in the Middle East oldest oil refinery zone soils: Source apportionment, speciation, bioaccessibility and human health risk assessment. *Environ. Sci. Pollut. Res.* **2020**, *27*, 40573–40591. [[CrossRef](#)]
106. Fang, F.; Wang, H.; Lin, Y. Spatial distribution, bioavailability, and health risk assessment of soil Hg in Wuhu urban area, China. *Environ. Monit. Assess.* **2011**, *179*, 255–265. [[CrossRef](#)]
107. Lin, H.; Zhu, X.; Feng, Q.; Guo, J.; Sun, X.; Liang, Y. Pollution, sources, and bonding mechanism of mercury in street dust of a subtropical city, southern China. *Hum. Ecol. Risk Assess. Int. J.* **2019**, *25*, 393–409. [[CrossRef](#)]
108. Sun, G.; Li, Z.; Bi, X.; Chen, Y.; Lu, S.; Yuan, X. Distribution, sources and health risk assessment of mercury in kindergarten dust. *Atmos. Environ.* **2013**, *73*, 169–176. [[CrossRef](#)]
109. Zhou, L.; Liu, G.; Shen, M.; Hu, R.; Sun, M.; Liu, Y. Characteristics and health risk assessment of heavy metals in indoor dust from different functional areas in Hefei, China. *Environ. Pollut.* **2019**, *251*, 839–849. [[CrossRef](#)]
110. Tashakor, M.; Modabberi, S. Human Health Risks Associated with Potentially Harmful Elements from Urban Soils of Hamedan City, Iran. *Pollution* **2021**, *7*, 709–722. [[CrossRef](#)]
111. Hou, S.; Zheng, N.; Tang, L.; Ji, X.; Li, Y.; Hua, X. Pollution characteristics, sources, and health risk assessment of human exposure to Cu, Zn, Cd and Pb pollution in urban street dust across China between 2009 and 2018. *Environ. Int.* **2019**, *128*, 430–437. [[CrossRef](#)]
112. Fernandes Azevedo, B.; Barros Furieri, L.; Peçanha, F.M.; Wiggers, G.A.; Frizzera Vassallo, P.; Ronacher Simões, M.; Fiorim, J.; de Batista, P.R.; Fioresi, M.; Rossoni, L. Toxic effects of mercury on the cardiovascular and central nervous systems. *J. Biomed. Biotechnol.* **2012**, 949048. [[CrossRef](#)]
113. Ghanavati, N.; Nazarpour, A.; De Vivo, B. Ecological and human health risk assessment of toxic metals in street dusts and surface soils in Ahvaz, Iran. *Environ. Geochem. Health* **2019**, *41*, 875–891. [[CrossRef](#)]
114. Morman, S.A.; Plumlee, G.S. The role of airborne mineral dusts in human disease. *Aeolian Res.* **2013**, *9*, 203–212. [[CrossRef](#)]
115. Antoniadis, V.; Shaheen, S.M.; Levizou, E.; Shahid, M.; Niazi, N.K.; Vithanageh, M.; Oki, Y.S.; Bolanj, N.; Rinklebe, J. A critical prospective analysis of the potential toxicity of trace element regulation limits in soils worldwide: Are they protective concerning health risk assessment?—A review. *Environ. Int.* **2019**, *127*, 819–847. [[CrossRef](#)]
116. Zittis, G.; Hadjinicolaou, P.; Lelieveld, J. Role of soil moisture in the amplification of climate warming in the eastern Mediterranean and the Middle East. *Clim. Res.* **2014**, *59*, 27–37. [[CrossRef](#)]